Tribological characterization of friction stir welded dissimilar aluminum alloy AA6061–AA5083 reinforced with CeO_2 and La_2O_3 nanoparticles

Arun M.
Department of Mechanical Engineering, N.S.N College of Engineering and Technology, Karur, India
Muthukumaran M.
Department of Mechanical Engineering, Jansons Institute of Technology, Coimbatore, India, and
Balasubramanian S.
Department of Mechanical Engineering, Kumaraguru College of Technology, Coimbatore, India

Abstract

Purpose – Dissimilar materials found applications in the structural fields to withstand the different types of loads and provide multi-facet properties to the final structure. Aluminum alloy materials are mostly used in aerospace and marine industries to provide better strength and safeguard the material from severe environmental conditions. The purpose of this study is to develop new material with superior strength to challenge the severe environmental conditions.

Design/methodology/approach – In the present investigation, friction stir welding (FSW) dissimilar joints were prepared from AA6061 and AA5083 aluminum alloys, and the weld nugget (WN) was reinforced with hard reinforcement particles such as La_2O_3 and CeO_2. The tribological and mechanical properties of the prepared materials were tested to analyze the suitability of material in the aerospace and marine environmental conditions.

Findings – The results showed that the AA6061–AA5083/La_2O_3 material exhibited better mechanical and tribological characteristics. The FSW dissimilar AA6061–AA5083/La_2O_3 material exhibited lower wear rate of 7.37×10^{-3} mm3/m and minimum friction coefficient of 0.31 compared to all other materials owing to the reinforcing effect of La_2O_3 particles and the fine grains formed by FSW process at WN region. Further, FSW dissimilar AA6061–AA5083/La_2O_3 material displayed a maximum tensile strength and hardness of 378 MPa and 118 HV, respectively, among all the other materials tested.

Originality/value – This work is original and novel in the field of materials science engineering focusing on tribological characteristics of friction stir welded dissimilar aluminum alloys by the reinforcing effect of hard particles such as La_2O_3 and CeO_2.

Keywords Mechanical properties, Friction stir welding, Tribological properties, Cerium oxide, Lanthanum oxide, AA5083 aluminum alloy, AA6061 aluminum alloy

Paper type Research paper

1. Introduction

Aluminum alloy is an alloy material consisting of Al as the predominant element and other elements such as Mg, Cu, Si, Mn and Sn are majorly presented in it. Aluminum alloys are attracted in the aerospace industries to manufacture the skin of aircraft and helicopter due to its high strength to weight ratio. Among the aluminum alloys, the AA6061 alloy is a precipitate hardened material having good mechanical properties with better weld characteristics. The AA6061 alloy is used in the construction of aircraft structure, automotive components, bicycle frame, etc. The aluminum alloy AA5083 is another alloy material that has better resistance against sea water and chemical attack. Hence, these materials are found applicable in the marine industries for ship and boat construction. Further, these materials are attracted in the areas where corrosion is to be eliminated such as railway road car, pressure vessel and drilling rigs.

Dissimilar welding is the joining of two materials with different chemical compositions. In the engineering field, it is required to join the combination of different characteristics material to achieve better end results. Recently, more research works have been performed on the dissimilar material (Abolusoro and Akinlabi, 2021; Ahmed *et al.*, 2021; Rabby *et al.*, 2021) and achieved better end results. For example, Jaiswal *et al.* (2021) performed a study on AA2014 and AA7075 joined by friction stir spot welding. Authors reported

The current issue and full text archive of this journal is available on Emerald Insight at: **https://www.emerald.com/insight/0036-8792.htm**

Industrial Lubrication and Tribology

[DOI 10.1108/ILT-01-2021-0009]

Received 18 January 2021
Revised 22 March 2021
24 April 2021
Accepted 26 April 2021

that the nugget zone, thermo-mechanically affected zone (TMAZ) and heat-affected zone (HZ) experienced significant changes in the grain size. Further, authors concluded that maximum shear strength of 4.15 kN was observed at the weld joint. Moreover, few authors have tried reinforcement particles in the preparation of dissimilar material (Saravanan *et al.*, 2020; Robin *et al.*, 2020). Anand and Sridhar (2020) investigated the effect of SiC and Al_2O_3 on the mechanical and microstructure properties of AA7075 and AA7475 aluminum alloy materials. The report showed that the AA7075–AA7475 dissimilar material with 2 Wt.% SiC displayed the maximum tensile strength and hardness of 191 MPa and 220 HV, respectively. Further, authors reported that friction stir welding (FSW) dissimilar material exhibited better results after including SiC particles due to its high hardness and grain refinement ability. Based on the literature survey conducted on FSW dissimilar aluminum alloy materials, it was concluded that the introduction of reinforcement particles improved the strength of the parent materials to a significant amount.

Lanthanum oxide (La_2O_3) is a solid white powder, odorless and insoluble in water, which is used in optical industry to manufacture high-precision glass and chemical product in automobile exhaust catalysts. Cerium oxide (CeO_2) is a rare earth element and yellow-whitish in color. It is used in the fuel cell, optics, polishing and biomedical applications. As lanthanum oxide and cerium oxide particles have played a significant role in the strengthening of properties of aluminum alloy-based composites (Srinivasan *et al.*, 2020; Kumar *et al.*, 2020), it is expected that these particles have the potential to improve the strength of the dissimilar aluminum alloys.

As the AA6061 alloy has the better mechanical strength and the AA5083 alloy provides good corrosion resistance, the combination of these two alloy material would provide a novel material with enhanced properties, and this could provide new information to the scientific society. Very limited studies are available in literature about the FSW of AA6061–AA5083. One study done by Devaiah *et al.* (2017) showed that welding speed of 80 mm/min exhibited good mechanical properties of joint compared to other welding speed. Another one study performed by Jannet *et al.* (2014) revealed that FSW of AA6061–AA5083 joint showed better mechanical properties than fusion welding of same material, and further, the weld profile displayed narrower structure. Hence, the literature survey on FSW of AA6061–AA5083 material reported that no study dealt with the reinforcement particles. Hence, there exists a research gap to use the hard reinforcement particles in the FSW of dissimilar material. Consequently, in this investigation, it is planned to strengthen the FSW AA6061–AA5083 joint by La_2O_3 and CeO_2 particles. The aim of this study is to fabricate the FSW AA6061–AA5083 joint by reinforcing with La_2O_3 and CeO_2 particles and analyze the tribological characteristics.

2. Materials and methods

In this investigation, the aluminum alloy materials AA6061 and AA5083 were used as base materials in the form of plates of dimensions 200 × 100 × 6 mm. The plates were supplied by Shree Sambhav Alloys, Mumbai, India. The La_2O_3 and CeO_2 nanoparticles were used as reinforcements in the FSW process. Nanoparticles were procured from Yaavik Materials & Engineering Private Limited, Telangana, India. The chemical compositions and properties of materials used are detailed in Tables 1 and 2, respectively. Before processing, FSW trials were performed to optimize the process parameters for defect free weld. FSW was performed for butt joint configuration and the processing parameters such as feed rate of 0.75 mm/s, piercing depth of 5.3 mm and spindle speed of 1,000 rpm were used. A groove was made at the edges of work pieces to fill the reinforcement particles before welding. The schematic diagram of experimental setup, groove dimension and FSW tool pin profile are shown in Figures 1 and 2(a) 2(b), respectively. A constant tool rotational speed of 1,000 rpm and a traverse speed of 45 mm/min were maintained throughout the experiment. The experiment was conducted at single pass of the tool and the work piece was allowed to cool at the room temperature after finishing welding. Tensile test specimen was cut across the weld direction. The test was performed on universal testing machine according to the standard ASTM E8/E8M-011 in room temperature, and the crosshead speed was maintained as 1 mm/min. The Vickers microhardness test was performed perpendicular to the weld direction by applying 100 g weight for a dwell time of 10 s. Wear test was performed on pin-on-disc tribometer using a pin of diameter 10 mm and length 30 mm. The wear test specimen was cut along the weld direction and the test was performed according to the standard ASTM G99-04. The parameters such as track diameter, load, sliding velocity and sliding distance were maintained as 100 mm, 50 N, 1.5 m/s and 1,000 m, respectively, in the wear test. The wear rate and wear resistance (Das *et al.*, 2020) were calculated using equations (1) and (2), respectively. The friction coefficient was calculated by measuring the forces using sensors in the tribometer setup:

$$\text{Wear rate } \left(\text{mm}^3/\text{m}\right) = \frac{Volume\ \ loss}{Sliding\ \ distance} \tag{1}$$

$$\text{Wear resistance } \left(\text{m}/\text{mm}^3\right) = \frac{1}{Wear\ \ rate} \tag{2}$$

3. Results and discussion

3.1 Tribological characterization

3.1.1 Wear rate and wear resistance

Figures 3(a) shows the results of wear rate and wear resistance of as-received base materials, FSW similar, FSW dissimilar and FSW dissimilar with reinforcement particles.

Table 1 Chemical composition of base materials

Aluminum alloy	Chemical compositions (Wt.%)									
	Si	Fe	Cu	Mn	Mg	Cr	Ni	Zn	Ti	Al
6061	0.615	0.304	0.258	0.045	0.901	0.19	0.013	0.054	0.0195	97.6
5083	0.076	0.13	0.032	0.63	4.34	0.064	0.003	0.035	0.055	94.6

Table 2 Properties of base materials and nanoparticles

Property	AA5083	AA6061	CeO_2	La_2O_3
Density (kg/m^3)	2,650	2,700	7,600	6,510
Melting point (°C)	570	588	2,340	2,315
Modulus of elasticity (GPa)	68	69	34	37
Tensile strength (MPa)	330	340	–	–
Brinell hardness	90	95	257	342

The base material displayed higher wear rate and the FSW dissimilar with reinforcement particles showed lower wear rate. Further, the FSW similar and dissimilar material exhibited lesser wear rate compared to base material. This is achieved by the development of fine grains at the weld nugget (WN) region due to the FSW effect. The fine grains improved the hardness of material by involving in the better stress transfer. Hence, the FSW materials of both similar and dissimilar displayed less wear rate than the as-received base materials. Moreover, the particle-reinforced FSW material showed the minimum wear rate compared to all other material because of the distribution of particles in the base material that restricted the growth of grain size and maintained the grain size as minimum as possible. This phenomenon assisted in the improvement of hardness of material. Hence, the FSW material with particle reinforcement showed least wear rates. In addition, among the particle reinforced FSW material, the AA6061–AA5083/La_2O_3 showed the minimum wear rate of 7.37×10^{-3} mm^3/m, which is 16.25% lower than the wear rate of AA6061–AA5083/CeO_2. This behavior was observed due to the high hardness of La_2O_3 particles compared to CeO_2 particles. Furthermore, the FSW of dissimilar AA6061–AA5083 material in presence of La_2O_3 nanoparticles significantly reduced the wear rate by 33% that could increase the life span of material and decrease the maintenance cost.

The FSW dissimilar material with reinforcement particles showed the superior wear resistance compared to FSW dissimilar without particle, FSW similar and base materials. When FSW was performed, the region nearer to weld tool experienced plastic deformation due to the heat, and recrystallization of structure occurred. The dynamic recrystallization of structure decreased the grain size which in turn decreased the microporosity of material. This behavior assisted in the improvement of wear resistance by providing

Figure 2 Schematic diagram of groove (a) FSW tool pin profile (b)

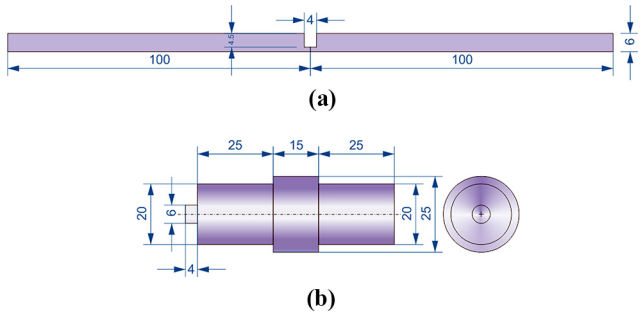

resistance force against the moving parts. Further, the inclusion of hard reinforcement particles such as La_2O_3 and CeO_2 in AA6061–AA5083 while performing FSW exhibited greater wear resistance compared to FSW dissimilar without particles. Owing to the addition of hard reinforcement particles, the particles were uniformly distributed in the weld zone, filled the gap between the atoms of base material and increased the dislocation density. Hence, the hardness of material was enhanced, which resulted in the improved wear resistance. Further, the FSW dissimilar AA6061–AA5083/La_2O_3 material showed the improvement in wear resistance by 22.12%, 69.61%, 49.25% and 19.4% compared to AA6061–AA6061, AA5083–AA5083, AA6061–AA5083 and AA6061–AA5083/CeO_2 materials, respectively.

3.1.2 Weight loss

Figure 3(b) shows the weight loss results of various tool pins of as-received base materials, FSW similar, FSW dissimilar and FSW dissimilar with reinforcement particles. The weight loss profile followed the similar trends of variation as wear rate profiles of various materials. The as-received base material showed more weight loss compared to all other materials because of the absence of reinforcing effect. The FSW similar and dissimilar material displayed lower weight loss compared to base material owing to the FSW effect at weld centre. During FSW, the coarse grain boundary was converted into fine grain boundary at WN that provided more resisting force against the movement of grains. Hence, the FSW material experienced lesser weight loss compared to base materials. Further, the FSW material with particle reinforcement showed minimum

Figure 1 Schematic diagram of experimental setup

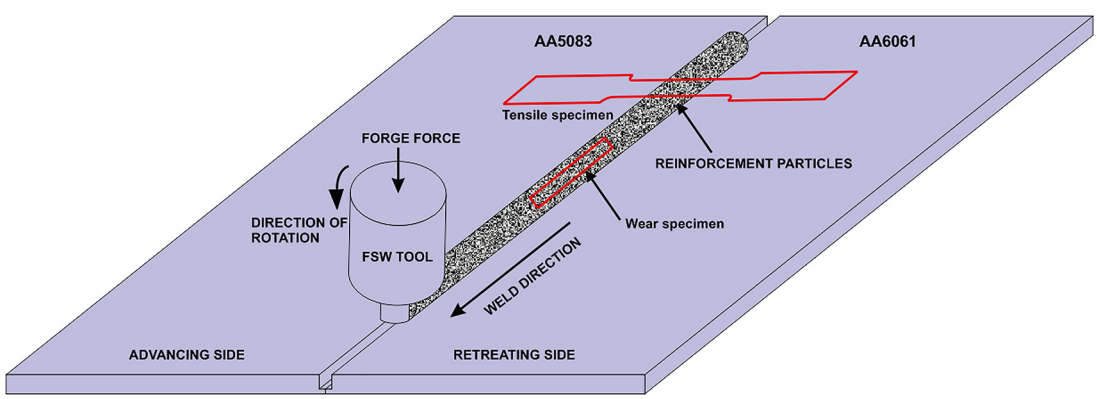

Figure 3 (a) Wear rate and wear resistance of BM and different types of FSW joints; (b) weight losses of BM and different types of FSW joints and (c) average friction coefficients of BM and different types of FSW joints

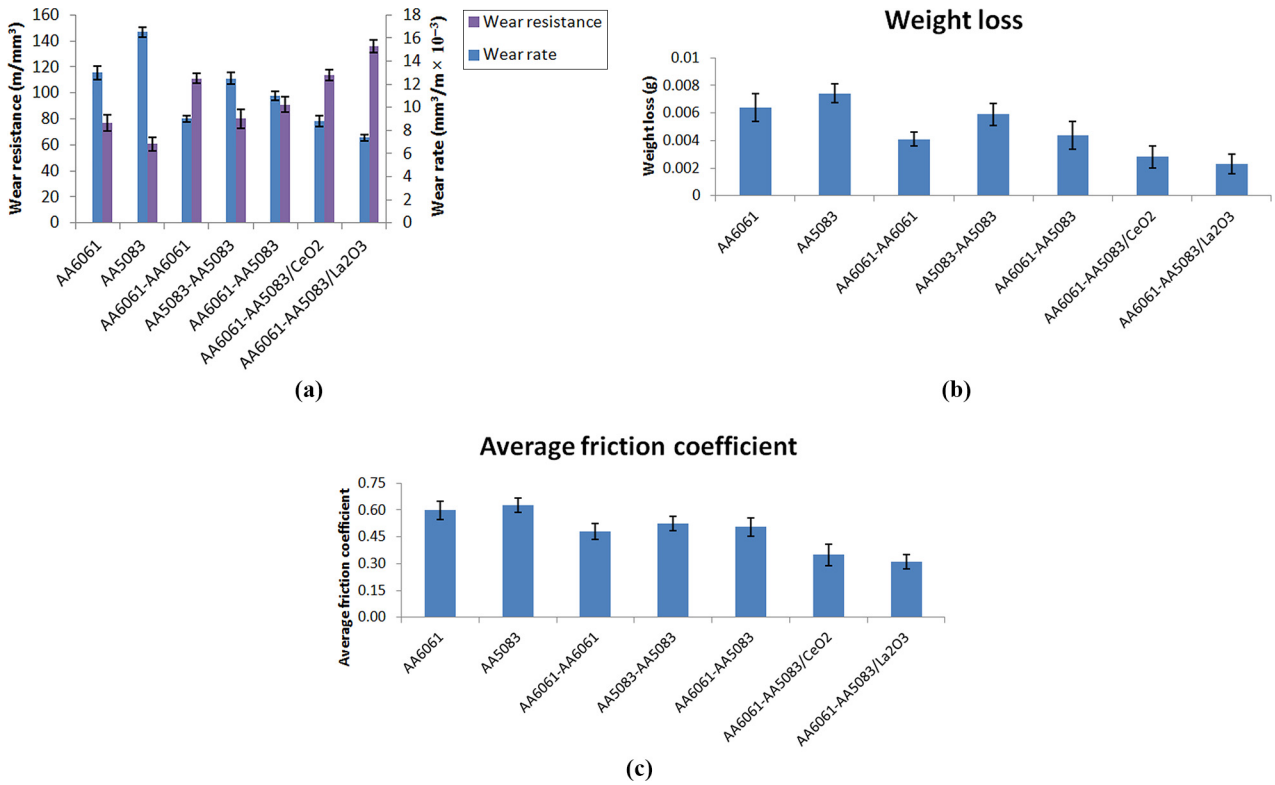

weight loss compared to FSW material without particle reinforcement and base materials. In case of FSW material with particle reinforcement, the particles were occupied in the space between the atoms of base material and increased the hardness of joint, which resulted in the least weight loss. Further, the AA6061–AA5083/La_2O_3 material displayed a minimum weight loss of 0.00231 g, which is the lowest weight loss observed in this study. This could be because of the combined effect of FSW of material and the reinforcing effect of hard La_2O_3 particles. Furthermore, the developed AA6061–AA5083/La_2O_3 material exhibited 47% decrement in the weight loss compared to that of FSW dissimilar AA6061–AA5083 material. Hence, nearly 50% of the material loss was saved due to the inclusion of La_2O_3 particle while performing FSW of AA6061–AA5083 material.

3.1.3 Average friction coefficient

Figure 3(c) shows the average friction coefficient values of various materials tested in this investigation. The base material AA6061 and AA5083 aluminum alloys showed the higher friction coefficient, and the FSW dissimilar material with particle reinforcement displayed the lower friction coefficient. Hence, the FSW process and the introduction of hard reinforcement particles decreased the friction coefficient because of the higher hardness and lower wear rate of materials. The reinforcement particles acted as the load bearing member and provided the lubricant effect to the FSW dissimilar material. Further, the FSW similar and dissimilar material exhibited lower friction coefficient values than base materials because of the welding effect that modified the crystal structure and grain size because of the plastic deformation that occurred with the help of heat generated while performing FSW process. In this investigation, the FSW dissimilar material AA6061–AA5083/La_2O_3 exhibited a minimum friction coefficient of 0.31 compared to all other material because of the reinforcing effect offered by the high hardness La_2O_3 particles.

3.2 Mechanical characterization

3.2.1 Tensile strength

Figure 4(a) shows the tensile strength results of base material and different types of FSW materials. The FSW materials, i.e. AA6061–AA6061, AA5083–AA5083, AA6061–AA5083 and AA6061–AA5083/CeO_2 and AA6061–AA5083/La_2O_3 showed the higher tensile strengths compared to base materials. When performing FSW, the base material was softened and experienced plastic deformation & grain refinement due to the heat generated during welding. The grain refinement assisted in the increase of grain dislocation density that led to the enhancement of hardness of materials. Hence, the tensile properties of FSW material displayed higher value than that of base materials. Further, the FSW material with particle reinforcements exhibited greater improvement in the tensile properties compared to FSW material without particle reinforcement. The reinforcement particles acted as a resistance provider for the deterioration in the base materials because of the pinning effect and hence increased the tensile strength of the materials. Moreover, the FSW material AA6061–AA5083/La_2O_3 showed the maximum tensile strength of 378 MPa and Young's modulus of 73 MPa compared to all the materials investigated. Similar type of work was done by Dragatogiannis *et al.* (2016). They performed friction stir welding

Figure 4 (a) Tensile strengths of BM and different types of FSW joints and (b) microhardness profile of FSW AA5083–AA6061 dissimilar joints

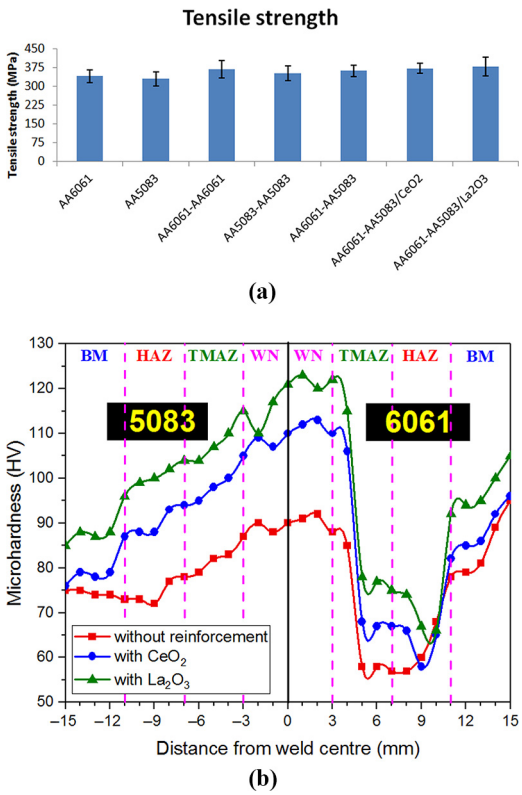

on AA5083–AA6082 on alloy by reinforcing with TiC particles and reported that the ultimate tensile strength of sample was increased from 193 MPa to 199 MPa after particle reinforcement.

3.2.2 Microhardness

Figure 4(b) shows the microhardness of profile of FSW AA6061–AA5083 dissimilar material. The hardness profile showed higher value at WN region and lower values at TMAZ, HZ and base metal (BM) regions. The WN zone displayed higher hardness value because of the grain refining effect by the FSW process. According to Hall–Petch relation, the hardness of structure increases with lower grain size (Bahrami *et al.*, 2014). The FSW process modified and decreased the grain size at WN region. Hence, the hardness value at WN zone showed higher value. Further, TMAZ and HZ exhibited lower hardness value compared to WN region where plastic deformation did not occur and the heat transfer only happened. Hence, the grain refinement was not achieved, which resulted into lower hardness value. Moreover, the TMAZ and HZ of AA6061 exhibited lower hardness value compared to that of AA5083 side owing to the dissolution of precipitates. In addition, the FSW dissimilar with particle reinforcement displayed higher hardness value compared to FSW dissimilar without reinforcement particles because of the high hardness of particles. This behavior is well in accordance with the previous research carried out by Pantelis *et al.* (2016). He performed friction stir welding on AA5083 and AA6082 with the assistance of SiC particle reinforcement and found that the hardness of SiC particle reinforced specimen was improved from 70 HV to 81 HV due to the particle addition. In this study, the FSW dissimilar AA6061-AA5083/La_2O_3 material showed the maximum hardness of 118 HV at WN region. This is 8.3% & 32.6% higher than AA6061–AA5083/CeO_2 & AA6061–AA5083 materials respectively. This could be because of the high hardness of La_2O_3 particles. Similar behavior was observed while comparing the hardness profile of FSW dissimilar AA6061–AA5083/CeO_2 with AA6061–AA5083. The FSW dissimilar AA6061–AA5083/CeO_2 showed the average hardness value of 110 HV, whereas the AA6061–AA5083 material exhibited 89 HV. The inclusion of CeO_2 particle in FSW dissimilar AA6061–AA5083 material restricted the grain growth by blocking the space between the atoms of AA6061 and AA5086 materials. This attributed to the improved hardness of AA6061–AA5083/CeO_2 material compared to AA6061–AA5083 material.

3.3 Surface morphology of worn-out surfaces

Morphological analysis of FSW dissimilar material with and without reinforcement was performed and presented in Figure 5. The FSW dissimilar AA6061–AA5083 showed more grooves, delaminating surfaces and wear debris compared to FSW dissimilar material with reinforcement particles because of un-reinforcing effect as discussed earlier. Further, the AA6061–AA5083/La_2O_3 displayed smooth grooves without delaminating surfaces and least wear debris compared to AA6061–AA5083/CeO_2 and AA6061–AA5083 materials owing to the lower wear rate experienced by the material because of the presence of hard La_2O_3 particles that provided sufficient strength to the material.

Figure 5 Scanning electron microscope images of worn-out surfaces

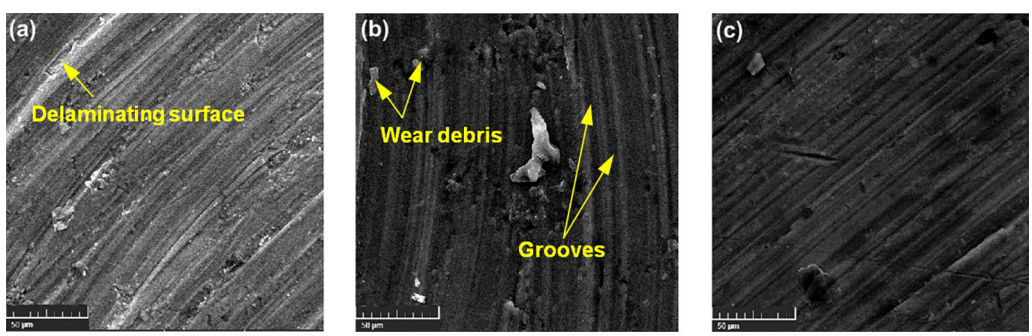

Notes: (a) AA6061–AA5083; (b) AA6061–AA5083/CeO_2; (c) AA6061–AA5083/La_2O_3

4. Conclusion

In the present investigation, friction stir welded dissimilar AA6061-AA5083 aluminum alloy joints were prepared, and the tribological and mechanical properties were studied. The following conclusions were derived from this study:

- The FSW dissimilar material AA6061–AA5083/La_2O_3 showed lower wear rate of 7.37×10^{-3} mm^3/m compared to all other materials due the formation of fine grain and the improvement in hardness by the hard La_2O_3 particles.
- The FSW dissimilar AA6061–AA5083/La_2O_3 displayed an improvement in the wear resistance by 22.12%, 69.61%, 49.25% and 19.4% compared to AA6061–AA6061, AA5083–AA5083, AA6061–AA5083 and AA6061–AA5083/CeO_2 materials, respectively.
- The FSW dissimilar material AA6061–AA5083/La_2O_3 exhibited a minimum friction coefficient of 0.31 compared to all other material because of the reinforcing effect offered by the high hardness La_2O_3 particles.
- The FSW dissimilar AA6061–AA5083/La_2O_3 material showed the maximum hardness of 118 HV at WN region. This is 8.3% & 32.6% higher than AA6061–AA5083/CeO_2 & AA6061–AA5083 materials respectively. This could be due to the high hardness of La_2O_3 particles.

References

Abolusoro, O.P. and Akinlabi, E.T. (2021), "Effects of processing parameters on temperature distributions, tensile behaviour and microstructure of friction stir welding of dissimilar aluminium alloys", *Trends in Manufacturing and Engineering Management*, pp. 721-733.

Ahmed, M.M., Ataya, S., El-Sayed Seleman, M.M., Mahdy, A., Alsaleh, N.A. and Ahmed, E. (2021), "Heat input and mechanical properties investigation of friction stir welded AA5083/AA5754 and AA5083/AA7020", *Metals*, Vol. 11 No. 1, p. 68.

Anand, R. and Sridhar, V.G. (2020), "Effects of SiC and Al 2 O 3 reinforcement of varied volume fractions on mechanical and micro structure properties of interlock FSW dissimilar joints AA7075-T6-AA7475-T7", *Silicon*, pp. 1-13.

Bahrami, M., Dehghani, K. and Givi, M.K.B. (2014), "A novel approach to develop aluminum matrix nano-composite employing friction stir welding technique", *Materials & Design*, Vol. 53, pp. 217-225.

Das, U., Das, R. and Toppo, V. (2020), "Dry sliding wear behavior study on friction stir weld joints of dissimilar aluminum alloys", *Materials Today: Proceedings*, Vol. 26, pp. 1815-1821.

Devaiah, D., Kishore, K. and Laxminarayana, P. (2017), "Effect of welding speed on mechanical properties of dissimilar friction stir welded AA5083-H321 and AA6061-T6 aluminum alloys", *International Journal of Advanced Engineering Research and Science*, Vol. 4 No. 3, pp. 22-28.

Dragatogiannis, D.A., Koumoulos, E.P., Kartsonakis, I.A., Pantelis, D.I., Karakizis, P.N. and Charitidis, C.A. (2016), "Dissimilar friction stir welding between 5083 and 6082 Al alloys reinforced with TiC nanoparticles", *Materials and Manufacturing Processes*, Vol. 31 No. 16, pp. 2101-2114.

Jaiswal, S., Verma, V. and Sharma, C. (2021), "Dissimilar friction stir spot welding of AA2014 and AA7075 aluminum alloys", *Recent Advances in Mechanical Engineering*, pp. 567-573.

Jannet, S., Mathews, P.K. and Raja, R. (2014), "Comparative investigation of friction stir welding and fusion welding of 6061 T6–5083 O aluminum alloy based on mechanical properties and microstructure", *Bulletin of the Polish Academy of Sciences Technical Sciences*, Vol. 62 No. 4, pp. 791-795.

Kumar, N., Navin, K., Ball, R.J. and Kurchania, R. (2020), "Mechanical and structural properties of aluminium nanocomposites reinforced with cerium oxide nanoparticles fabricated by powder metallurgy", *Journal of Materials NanoScience*, Vol. 7 No. 2, pp. 73-78.

Pantelis, D.I., Karakizis, P.N., Daniolos, N.M., Charitidis, C.A., Koumoulos, E.P. and Dragatogiannis, D.A. (2016), "Microstructural study and mechanical properties of dissimilar friction stir welded AA5083-H111 and AA6082-T6 reinforced with SiC nanoparticles", *Materials and Manufacturing Processes*, Vol. 31 No. 3, pp. 264-274.

Rabby, R.E., Olszta, M.J., Overman, N.R., Mcdonnell, M. and Whalen, S.A. (2021), "Friction stir dovetailing of AA7099 to steel with AA6061 interlayer for reduced Zn embrittlement at dissimilar interface", *Journal of Manufacturing Processes*, Vol. 61, p. 155326.

Robin, L.G., Raghukandan, K. and Saravanan, S. (2020), "Studies on wire-mesh and silicon carbide particle reinforcements in explosive cladding of Al 1100-Al 5052 sheets", *Journal of Manufacturing Processes*, Vol. 56, pp. 887-897.

Saravanan, S., Inokawa, H., Tomoshige, R. and Raghukandan, K. (2020), "Microstructural characterization of silicon carbide reinforced dissimilar grade aluminium explosive clads", *Defence Technology*, Vol. 16 No. 3, pp. 689-694.

Srinivasan, S.A., Babu, S.K., Thirumaran, B. and Vallimanalan, A. (2020), "Wear behavioral and mechanical studies on liquid forged VAL12 alloy strengthened by lanthanum oxide dispersoids", *Journal of The Institution of Engineers (India): Series D*, pp. 1-14.

Corresponding author

Arun M. can be contacted at: arunmphd@gmail.com